Istanbul Technical University
Faculty of Aeronautics and Astronautics
Aeronautical Engineering Department

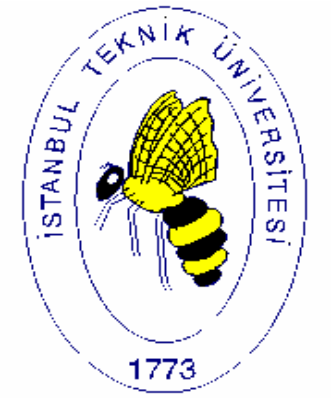

Flight Stability and Control
Project Report

Longitudinal Stability of Learjet 24 Business Aircraft

Prepared By # Tevfik Uyar, 110030015
Instructor: Prof. Dr. Elbrus Caferov

CONTENTS

Learjet 24

Summary:

Stability includes how an aircraft responds to changes in its position such as angle of attack, slip or bank. Control refers to the ability to initiate and sustain changes in same parameters. That has to be recognised the character of an aircraft opposite to change of its position for a securefull flight.

In this project, not only longitudinal stability of Learjet 24 business jet is investigated but also given some information about it. Some supported materials and computer languages / softwares used to do job such as Mathematica and MatLab.

There is a conclusion part at the last chapter to see the summary of results added to conclusion. Have a good read!

1. Basic Information for Learjet 24 Aircraft

1.1 History

Mention the phrase "private jet" to the average person and one word immediately pops into mind: Lear. Since its first flight in 1963, William P. Lear Sr.'s innovative aircraft, built to replicate the performance and amenities of a commercial airliner, has been tantamount with executive business travel.

One of the inventors of the 8-track audio tape, the holder of 150 aviation-related patents and a high school drop-out, Lear abandoned his retirement in Switzerland to establish the Swiss American Aircraft Company (SAAC). In 1959, SAAC began work on Lear's latest invention—a private luxurious jet aircraft with the flexibility to fly passengers and freight in and out of small airports around the world. Lear undertook his bold gamble without the benefit of a market survey to evaluate the consumer demand for such an aircraft, relying instead on pure intuition.

Inspired by a single-seat Swiss strike fighter aircraft, the FFA P-16 (flown as a prototype in April 1955 but never put into production), Lear recruited a group of Swiss aircraft designers and engineers to transform the fighter's wing and basic airframe design into the cornerstone of a revolutionary aircraft—originally designated as the SAAC-23 but soon renamed as the Learjet 23 Continental.

Problems with suppliers and production tooling in Switzerland compelled Lear to shift assembly of the new aircraft to Wichita, Kansas (under the new name of Lear Jet Industries), where the prototype Learjet 23 made its first flight on October 7, 1963, from Wichita's Mid-Continent Airport, nine months after work had begun on the project. The original Learjet accumulated 194 hours of flight time in 167 test flights until it was destroyed in June 1964 when it crashed at takeoff with a Federal Aviation Administration pilot at the controls. The cause of the accident was determined to be pilot error—retraction of the jet's lift spoilers was overlooked. However, a second prototype Learjet 23 soon received formal FAA certification on July 31, 1964.

The Learjet 23 became the first small jet aircraft to enter mass production as well as the first to be developed and financed by a single individual. Chemical and Industrial Corporation of Cincinnati, Ohio, took delivery of the first production Learjet on October 13, 1964, one year after its initial flight.

The undisputed marketing success of the Learjet 23 spurred development of a new aircraft with improved low-speed handling characteristics, coupled with increased range, size, and speed. Approximately 105 Learjet 23s were built from 1963 to 1966 until replaced by the improved Model 24 (the 150th Learjet built), which made its debut in March 1966.

1.2 Properties of Learjet 24

The all-metal fuselage of the Learjet 24 was a flush-riveted semi-monocoque design. It was equipped with wingtip fuel tanks that added 364 extra gallons (1,378 liters) of fuel capacity and featured the added attraction of a "T-tail" configuration.

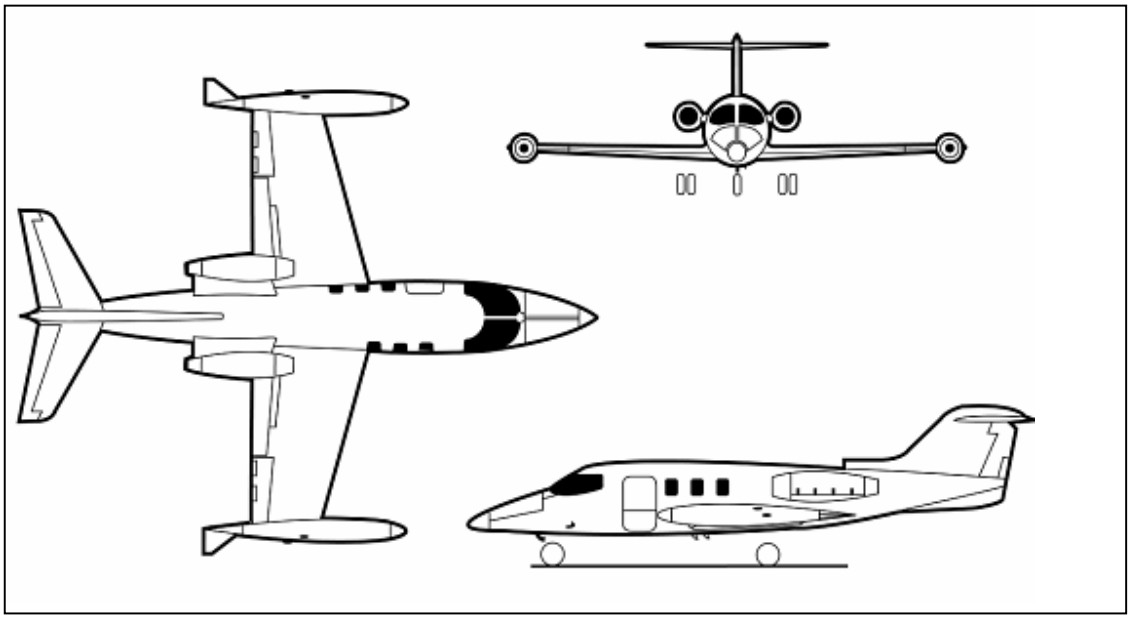

Figure 1.1: Sheme of Learjet 24

The high cruising altitude and long endurance flight capability of the Learjet also made it an ideal aircraft for target towing, photo-surveying, and high-altitude mapping. A number of foreign Air Forces, including Bolivia, Ecuador, Argentina, Mexico, Peru, and Yugoslavia, modified the corporate jet for military missions.

Picture 1.1: A Learjet 24

The Learjet, both as a technological innovation and a commercial success, is widely recognized as a trailblazer in the business jet industry. Few products, before or since, enjoy its instant name recognition.

General Characteristics of Learjet 24

- Cabin Height (Feet) 4.3
- Cabin Width (Feet) 4.9
- Cabin Length (Feet) 9
- Cabin Volume (Cubic Feet) 192
- Door Height (Feet) 4.2
- Door Width (Feet) 3
- Baggage Volume Internal (Cubic Feet) 40
- Baggage Volume External (Cubic Feet) n/a
- Seats - Executive 5
- Maximum Take-off Weight (lbs) 13500
- Maximum Landing Weight (lbs) 11880
- Basic Operating Weight w/crew (lbs) 7830
- Usable Fuel (lbs) 5628
- Payload with Full Fuel (lbs) 342

- Maximum Payload (lbs) 3570
- Range - Seats Full (nm) 850
- Maximum Range (nm) 1100
- Balance Field Length (feet) 4300
- Landing Distance (Factored) (feet) 5325
- Rate of Climb - ALL Engines (feet p/min) 6800
- Rate of Climb - One Engine Out (feet p/min) 2100
- Max Cruise Speed (ktas) 475
- Normal Cruise Speed (ktas) 439
- Long Range Cruise Speed (ktas) 410
- Service Ceiling at Maximum Weight (feet) 45000
- One Engine Inoperative Service Ceiling at Maximum Weight (feet) 28500
- Number of Engines 2
- Engine Model CJ610-6
- Engine Manufacturer General Electric
- Hover In Ground Effect (feet) n/a
- Hover Out of Ground Effect (feet) n/a

Table 1.1: General Characteristics for Learjet 24

$C_{D_u} = 0.104;$	$C_{M_u} = 0.05;$
$C_{D_1} = 0.0335;$	$C_{M_1} = 0;$
$C_{T_{x_u}} = -0.0700;$	$C_{M_{T_u}} = 0;$
$C_{T_{x_1}} = 0.0335;$	$C_{M_{T_1}} = 0;$
$C_{D_\alpha} = 0.3;$	$C_{M_\alpha} = -0.640;$
$C_{L_1} = 0.410;$	$C_{M_{T_\alpha}} = 0;$
$C_{D_{\delta_e}} = 0;$	$C_{M_{\dot{\alpha}}} = -6.70;$
$C_{L_u} = 0.400;$	$C_{M_q} = -15.5;$
$C_{L_1} = 0.410;$	$C_{M_{\delta_e}} = -1.240;$
$C_{L_\alpha} = 5.840;$	$S = 230;$
$C_{D_1} = 0.0335;$	$\bar{c} = 7;$
$C_{L_{\dot{\alpha}}} = 2.20;$	$U_1 = 677;$
$C_{L_q} = 4.7;$	$\bar{q} = 134.6;$
$C_{L_{\delta_e}} = 0.46;$	$W = 13000;$
	$I_{yy} = 18800;$
	$g = 32.174;$
	$\theta_1 = 0;$

Table 1.2: Non-dimensional Coefficients for Learjet 24

2. Introduction to Stability and Control

When it is talked about a flight with an aircraft; it includes many topics as a subset of broad range of challenging topics. Because an aircraft is not a rigid body and also uses some natural forces to lift in atmosphere. To fly securely, is a complex job and not very simple. It is really important to obtain information and use in all design phases about; aerodynamic performance, engines, structural issues, vehicle's dynamic and its control, and all issues contained by Flight Mechanics.

Also a vehicle design envelops all of these more basic issues. It involves integrating knowledge in each of the four subject areas in order to synthesize a complete vehicle which satisfies prescribed performance requirements. This topic is also referred to as flight mechanics. Flight mechanics comprises three major subtopics such as; Performance, Stability and control, Aeroelasticity.

As sum up, each of these subtopics is studied individually although they are combined to each other. While studying aircraft performance, it is directly related via the parameters like range, take-off and landing distance, and trajectory planning (mission profile) for a given aircraft. This involves determining the forces necessary to achieve a given path of motion, assuming that these desired forces can be generated. As a result, one typically models the aircraft as a point mass subject to three "control" forces: Lift, Side force, and Thrust.

While studying stability and control, lift and side forces are not true control forces. Actually, these forces are outcome of the aircraft's guidance referring to the air flow. For instance, the vehicle must attack with an angle to provide a lift force. Stability and control, researches how the vehicle's orientation, or attitude changes with moments generated by the control surfaces typically generated by the pilot or another systems attached to control. Moreover, control relates to a pilot's interaction with the aircraft and observes, how effective the various actuators are at forcing the aircraft into a desired motion and how much effort is required of the pilot to generate the necessary actuator commands?

When discussing flight of atmospheric vehicles, the term "stability" refers to a property of a special class of motion known as steady motion. For a vehicle in steady motion, all components of translational and angular velocity are constant. A special case of steady motion is equilibrium flight, in which the vehicle acceleration is zero. Note that these two definitions are distinct. Steady, wings-level flight at constant altitude is equilibrium flight. A horizontal turn at constant radius and velocity is not equilibrium flight; the constant yaw rate turn requires a constant centripetal acceleration. Both flight conditions are steady motions, however. Stability (or instability) is a property corresponding to a steady motion.

3. Longitudinal Stability

3.1 Introduction

Longitudinal stability refers to stability around the lateral axis. It is also called pitch stability. Longitudinal stability depends on the location of the center of gravity (c of g.) This is the most important thing to realize as a pilot. If the aircraft is loaded within the approved c of g envelope it will have positive static longitudinal stability. That is critical, because an aircraft with negative longitudinal stability would be impossible to fly for more than a few moments. It would require tremendous concentration to avoid over controlling such an aircraft.

Figure 3.1: Longitudinal Stability

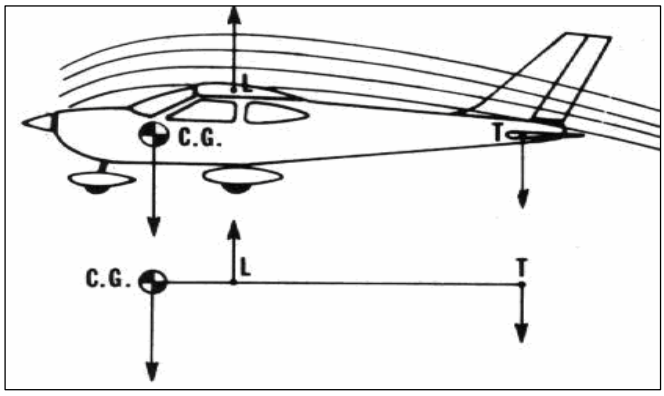

Just as with directional stability, longitudinal stability depends on the weather veining. The only complication is that for most aircraft there are two wings producing lift affecting the longitudinal stability, whereas the directional stability depended only upon one wing, the fin.

Additionally, longitudinal stability is compromised by the fact that the main wing must be close to the c of g since net lift must act opposite to weight. Conversely directional stability was easier to achieve because the fin was placed well behind the c of g and was not required to produce any force under normal flight conditions.

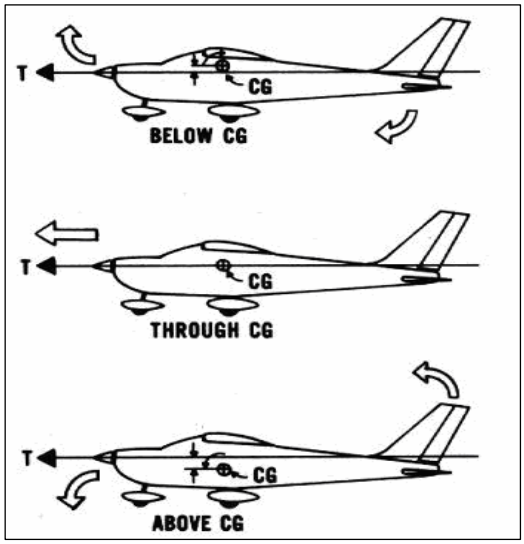

Figure 3.2: Longitudinal Stability Effects over Aircraft

From the above you can easily guess that the stabilizer must be a major contributor to longitudinal stability. This is in fact the case. Most aircraft would be completely unstable without the horizontal stabilizer. The stabilizer provides the same function in longitudinal stability as the fin does in directional stability. When the angle of attack changes it tends to pitch the aircraft back to its original angle of attack. The main wing, on the other hand, may be stable, or unstable, depending on the exact location of the CG.

3.2 Obtaining the Dimensional Parameters

Table 1.2 shows that, it is obtained non-dimensional parameters forthe Learjet 24 from the references. However, it will be used the dimensional parameters for it. So it has to be calculated by the formulas taken from references. It is used Matematica software to obtain them, as showed below:

$$X_u = -\frac{\bar{q} * S}{m * U_1} * (C_{D_u} + 2 * C_{D_1}) \qquad = -0.0193527$$

$$X_{T_u} = \frac{\bar{q} * S}{m * U_1} * (C_{T_{x_u}} + 2 * C_{T_{x_1}}) \qquad = -0.000339521$$

$$X_\alpha = \frac{\bar{q} * S}{m} * (-C_{D_\alpha} + C_{L_1}) \quad = 8.42805$$

$$X_{\delta_e} = -\frac{\bar{q} * S}{m} * C_{D_{\delta_e}} \quad = 0$$

$$Z_u = -\frac{\bar{q} * S}{m * U_1} * (C_{L_u} + 2 * C_{L_1}) \quad = -0.138072$$

$$Z_\alpha = -\frac{\bar{q} * S}{m} * (C_{L_\alpha} + 2 * C_{D_1}) \quad = -452.586$$

$$Z_{\dot{\alpha}} = -\frac{\bar{q} * S * \bar{c}}{2 * m * U_1} * C_{L_{\dot{\alpha}}} \quad = -0.871438$$

$$Z_q = -\frac{\bar{q} * S * \bar{c}}{2 * m * U_1} * C_{L_q} \quad = -1.86171$$

$$Z_{\delta_e} = -\frac{\bar{q} * S}{m} * C_{L_{\delta_e}} \quad = -35.2446$$

$$M_u = \frac{\bar{q} * S * \bar{c}}{I_{yy} * U_1} * (C_{M_u} + 2 * C_{M_1}) \quad = 0.000851323$$

$$M_{T_u} = \frac{\bar{q} * S * \bar{c}}{I_{yy} * U_1} * (C_{M_{T_u}} + 2 * C_{M_{T_1}}) \quad = 0$$

$$M_\alpha = \frac{\bar{q} * S * \bar{c}}{I_{yy}} * C_{M_\alpha} \quad = -7.37723$$

$$M_{T_\alpha} = \frac{\bar{q} * S * \bar{c}}{I_{yy}} * C_{M_{T_\alpha}} \quad = 0$$

$$M_{\dot{\alpha}} = \frac{\bar{q} * S * \bar{c}^2}{I_{yy} * 2 * U_1} * C_{M_{\dot{\alpha}}} \quad = -0.399271$$

$$M_q = \frac{\bar{q} * S * \bar{c}^2}{I_{yy} * 2 * U_1} * C_{M_q} = -0.923686$$

$$M_{\delta_e} = \frac{\bar{q} * S * \bar{c}}{I_{yy}} * C_{M_{\delta_e}} = -14.2934$$

3.2 Obtaining the Linearized Equation of Motion (EoM) in Laplace Form

For the EOM of aircraft, it is necessary to use power of Laplace Transforms.

$$\begin{aligned}
\dot{u} &= -g\theta\cos\Theta_1 + X_u u + X_{T_u} + X_\alpha \alpha + X_{\delta_e} \delta_e \\
\dot{w} - U_1 q &= -g\theta\sin\Theta_1 + Z_u u + Z_\alpha \alpha + Z_{\dot{\alpha}} \dot{\alpha} + Z_q q + Z_{\delta_e} \delta_e \\
\dot{q} &= M_u u + M_{T_u} u + M_\alpha \alpha + M_{T_\alpha} \alpha + M_{\dot{\alpha}} \dot{\alpha} + M_q q + M_{\delta e} \delta_e
\end{aligned} \quad \text{(Eq. 3.1)}$$

EOM have 5 aircraft motion variables: u, θ, α, w, q, δ_e however there are only 3 equations. It is necessary to reduce down the variables number. It will be used the dynamic equations of kinematic relation and the approximation for angle of attack, α to reduce to the three motion variables of α, u, θ.

$$q = \dot{\theta} \quad \dot{q} = \ddot{\theta}$$

$$\alpha \approx \frac{w}{U_1} \rightarrow w = \alpha U_1 \Rightarrow \dot{w} = \dot{\alpha} U_1$$

Therefore, aircraft motion variables are reduced to α, u and θ. These should be thought of as the outputs of system of differential equations. With zero initial conditions, the Laplace transform of Eq.3.1 yields:

$$su(s) = -g\theta(s)\cos\Theta_1 + X_u u(s) + X_{T_u} u(s) + X_\alpha \alpha(s) + X_{\delta_e} \delta_e(s)$$

$$sU_1\alpha(s) - U_1 s\theta(s) = -g\theta(s)\sin\Theta_1 + Z_u U(s) + Z_\alpha \alpha(s) + Z_{\dot{\alpha}} s\alpha(s) + Z_q s\theta(s) + Z_{\delta_e} \delta_e(s)$$

$$s^2\theta(s) = M_u u(s) + M_{T_u} u(s) + M_\alpha \alpha(s) + M_{T_\alpha} \alpha(s) + M_{\dot{\alpha}} s\alpha(s) + M_q s\theta(s) + M_{\delta_e} \delta_e(s)$$

Combining terms yields

$$X_{\delta_e}\delta_e(s) = (s - X_u - X_{T_u})u(s) - X_\alpha\alpha(s) + g\cos\Theta_1\theta(s)$$
$$Z_{\delta_e}\delta_e(s) = -Z_u u(s) + [(U_1 - Z_{\dot\alpha})s - Z_\alpha]\alpha(s) + [-(Z_q - U_1)s + g\sin\Theta_1]\Theta(s)$$
$$M_{\delta_e}\delta_e(s) = -(M_u - M_{T_u})u(s) - (M_{\dot\alpha}s + M_\alpha + M_{T_\alpha})\alpha(s) + (s^2 + M_q s)\theta(s)$$

δ_e (elevator deflection) terms oved to the left side, because δ_e is common forcing function (or input) for each of the three differential equations. In matrix form, this yields:

$$\begin{pmatrix} (s - X_u - X_{T_u}) & -X_\alpha & g\cos\Theta_1 \\ -Z_u & [s\,(U_1 - Z_{\dot\alpha}) - Z_\alpha] & [-(Z_q + U_1)\,s + g\sin\Theta_1] \\ -(M_u + M_{T_u}) & -[M_{\dot\alpha}\,s + M_\alpha + M_{T_\alpha}] & (s^2 - M_q\,s) \end{pmatrix} \begin{pmatrix} u(s) \\ \alpha(s) \\ \theta(s) \end{pmatrix} = \begin{pmatrix} X_{\delta_e} \\ Z_{\delta_e} \\ M_{\delta_e} \end{pmatrix} \delta_e(s)$$

In terms of transfer functions

$$\begin{pmatrix} (s - X_u - X_{T_u}) & -X_\alpha & g\cos\Theta_1 \\ -Z_u & [s\,(U_1 - Z_{\dot\alpha}) - Z_\alpha] & [-(Z_q + U_1)\,s + g\sin\Theta_1] \\ -(M_u + M_{T_u}) & -[M_{\dot\alpha}\,s + M_\alpha + M_{T_\alpha}] & (s^2 - M_q\,s) \end{pmatrix} \begin{pmatrix} \frac{u(s)}{\delta_e(s)} \\ \frac{\alpha(s)}{\delta_e(s)} \\ \frac{\theta(s)}{\delta_e(s)} \end{pmatrix} = \begin{pmatrix} X_{\delta_e} \\ Z_{\delta_e} \\ M_{\delta_e} \end{pmatrix}$$

They can be written as below with applying *Cramer Rule:*

$$\frac{u(s)}{\delta_e(s)} = \frac{\mathrm{Det}\begin{bmatrix} X_{\delta_e} & -X_\alpha & g \\ Z_{\delta_e} & (s*U_1 - Z_\alpha) & -U_1 s \\ M_{\delta_e} & -(M_{\dot\alpha} s + M_\alpha) & s^2 - M_q s \end{bmatrix}}{\mathrm{Det}\begin{bmatrix} (s - X_u - X_{T_u}) & -X_\alpha & g \\ -Z_u & (s*U_1 - Z_\alpha) & -U_1 s \\ -(M_u + M_{T_u}) & -(M_{\dot\alpha} s + M_\alpha) & s^2 - M_q s \end{bmatrix}}$$

(Eq. 3.2a)

$$\frac{\alpha(s)}{\delta_e(s)} = \frac{\mathrm{Det}\begin{bmatrix} (s - X_u - X_{T_u}) & X_{\delta_e} & g \\ -Z_u & Z_{\delta_e} & -U_1 s \\ -(M_u + M_{T_u}) & M_{\delta_e} & s^2 - M_q s \end{bmatrix}}{\mathrm{Det}\begin{bmatrix} (s - X_u - X_{T_u}) & -X_\alpha & g \\ -Z_u & (s*U_1 - Z_\alpha) & -U_1 s \\ -(M_u + M_{T_u}) & -(M_{\dot\alpha} s + M_\alpha) & s^2 - M_q s \end{bmatrix}}$$

(Eq. 3.2b)

$$\frac{\theta(s)}{\delta_e(s)} = \frac{\mathrm{Det}\begin{bmatrix} (s - X_u - X_{T_u}) & -X_\alpha & X_{\delta_e} \\ -Z_u & (s*U_1 - Z_\alpha) & Z_{\delta_e} \\ -(M_u + M_{T_u}) & -(M_{\dot\alpha} s + M_\alpha) & M_{\delta_e} \end{bmatrix}}{\mathrm{Det}\begin{bmatrix} (s - X_u - X_{T_u}) & -X_\alpha & g \\ -Z_u & (s*U_1 - Z_\alpha) & -U_1 s \\ -(M_u + M_{T_u}) & -(M_{\dot\alpha} s + M_\alpha) & s^2 - M_q s \end{bmatrix}}$$

(Eq. 3.2c)

Table 3.1: Transfer Functions

The characteristic equation is;

$$(s^2 + 2\,\zeta_{SP}\,\omega_{N_{SP}}\,s + \omega_{N_{SP}}{}^2)\;(s^2 + 2\,\zeta_{PH}\,\omega_{N_{PH}}\,s + \omega_{N_{PH}}{}^2) = 0$$

3.3 Obtaining the Transfer Functions and Natural Frequencies

$\boxed{\frac{u(s)}{\delta_e(s)}}$ Using the Equation 3.2a, it is found:

$$\frac{199768. + 229678.\,s - 297.043\,s^2}{45.1686 + 122.884\,s + 5426.41\,s^2 + 1361.64\,s^3 + 677.871\,s^4}$$

In simplified form

$$-\frac{0.4382\,(-774.084 + s)\,(0.868796 + s)}{(0.00837566 + 0.0206935\,s + s^2)\,(7.95556 + 1.988\,s + s^2)}$$

$\boxed{\frac{\alpha(s)}{\delta_e(s)}}$ Using the Equation 3.2b, it is found:

$$\frac{-64.4613 - 190.671\,s - 9683.25\,s^2 - 35.2446\,s^3}{45.1686 + 122.884\,s + 5426.41\,s^2 + 1361.64\,s^3 + 677.871\,s^4}$$

In simplified form

$$-\frac{0.051993\,(274.725 + s)\,(0.00665746 + 0.019668\,s + s^2)}{(0.00837566 + 0.0206935\,s + s^2)\,(7.95556 + 1.988\,s + s^2)}$$

$\boxed{\frac{\theta(s)}{\delta_e(s)}}$ Using the Equation 3.2c, it is found:

$$\frac{-139.155 - 6399.5\,s - 9675.\,s^2}{45.1686 + 122.884\,s + 5426.41\,s^2 + 1361.64\,s^3 + 677.871\,s^4}$$

In simplified form

$$-\frac{14.2726\,(0.0225107 + s)\,(0.638937 + s)}{(0.00837566 + 0.0206935\,s + s^2)\,(7.95556 + 1.988\,s + s^2)}$$

$$(s^2 + 2\,\zeta_{SP}\,\omega_{N_{SP}}\,s + \omega_{N_{SP}}{}^2)\;(s^2 + 2\,\zeta_{PH}\,\omega_{N_{PH}}\,s + \omega_{N_{PH}}{}^2) = 0$$

$$\omega_{N_{SP}} = \sqrt{7.955557384078312`} = 2.82056$$

$$\omega_{N_{PH}} = \sqrt{0.008375658050738992`} = 0.0915186$$

$$\zeta_{SP} = \frac{1.988003267288063`}{2\,\omega_{N_{SP}}} = 0.352413$$

$$\zeta_{PH} = \frac{0.020693521017890276`}{2\,\omega_{N_{PH}}} = 0.113056$$

3.4 Short Period Approximation

3.4.1 Obtaining the formulas for Short Period Approximation

It must be looked at a two degree of freedom approximation to gain inside into the stability parameters and derivatives that influence the dynamic characteristics of the short period mode. This is a solution in which the motion is constrained to two motion variables rather than three. Recalling discussion on the short period mode, it is maden the simplifying assumption that u remains constant and can be removed from above equations. With this assumption and the elimination of the x force equation (which is assumed to have a negligible affect if u is approximately constant), it is retained z force equation and the Pitching Moment equation along with the motion variables α and θ.

$$\begin{pmatrix} [s\,(U_1 - Z_{\dot\alpha}) - Z_\alpha] & [-(Z_q + U_1)\,s + g\sin\Theta_1] \\ -[M_{\dot\alpha}\,s + M_\alpha + M_{T_\alpha}] & (s^2 - M_q\,s) \end{pmatrix} \begin{pmatrix} \alpha\,(s) \\ \Theta\,(s) \end{pmatrix} = \begin{pmatrix} Z_{\delta_e} \\ M_{\delta_e} \end{pmatrix} \delta_e\,(s)$$

It is assumed that: $\boxed{Z_{\dot\alpha} = Z_q = \Theta_1 = M_{T_\alpha} = 0}$ because they are small enough to be negligible when compared with others. So; the new form of matrix is:

$$\begin{pmatrix} sU_1 - Z_\alpha & U_1 s \\ -[M_{\dot{\alpha}} s + M_\alpha] & s^2 - M_q s \end{pmatrix} \begin{pmatrix} \alpha(s) \\ \theta(s) \end{pmatrix} = \begin{pmatrix} Z_{\delta_e} \\ M_{\delta_e} \end{pmatrix} \delta_e(s)$$

The characteristic equation is:

$$(sU_1 - Z_\alpha)\left(s^2 - M_q s\right) - (U_1 s)\left(-[M_{\dot{\alpha}} s + M_\alpha]\right) = 0$$

Via Cramer Rule; the transfer functions $\alpha(s) / \delta_e(s)$ and $\theta(s)/ \delta_e(s)$ are:

$$\frac{\alpha(s)}{\delta_e(s)} = \frac{Z_{\delta_e} s + (M_{\delta_e} U_1 - M_q Z_{\delta_e})}{U_1\left(s^2 - \left(M_q + \frac{Z_\alpha}{U_1} + M_{\dot{\alpha}}\right) s + \left(\frac{Z_\alpha M_q}{U_1} - M_\alpha\right)\right)}$$

(Eq. 3.3a)

$$\frac{\theta(s)}{\delta_e(s)} = \frac{(U_1 M_{\delta_e} + Z_{\delta_e} M_{\dot{\alpha}}) s + (M_\alpha Z_{\delta_e} - Z_\alpha M_{\delta_e})}{sU_1\left(s^2 - \left(M_q + \frac{Z_\alpha}{U_1} + M_{\dot{\alpha}}\right) s + \left(\frac{Z_\alpha M_q}{U_1} - M_\alpha\right)\right)}$$

(Eq. 3.3b)

Table 3.2: Transfer Functions for Short Period Approximation

Natural Frequency and Damping Ratio can be approximated as:

$$\omega_{n_{SP}} \approx \sqrt{\frac{Z_\alpha M_q}{U_1} - M_\alpha} \qquad \zeta_{SP} \approx \frac{-\left(M_q + \frac{Z_\alpha}{U_1} + M_{\dot{\alpha}}\right)}{2\omega_{n_{SP}}}$$

3.4.2 Obtaining the numerical results for Short Period Approximation

$\frac{\alpha(s)}{\delta_e(s)}$ Using the Equation 3.3a, it is found:

$$\frac{-9709.17 - 35.2446\, s}{677\,(7.99473 + 1.99147\, s + s^2)}$$

In simplified form

$$\frac{-14.3415-0.05206\,s}{7.99473+1.99147\,s+s^2}$$

$\boxed{\frac{\theta(s)}{\delta_e(s)}}$ Using the Equation 3.3b, it is found:

$$\frac{-6208.98-9662.54\,s}{677\,s\,(7.99473+1.99147\,s+s^2)}$$

In simplified form

$$\frac{-9.17132-14.2726\,s}{s\,(7.99473+1.99147\,s+s^2)}$$

Characteristic Equation;

$$(sU_1 - Z_\alpha)\left(s^2 - M_q\,s\right) - (U_1\,s)\,(-[M_{\dot{\alpha}}\,s + M_\alpha]) = 0$$

$$677\,(7.37723+0.399271\,s)\,s + (452.586+677\,s)\,(0.923686\,s+s^2) = 0$$

In simplified form

$$s\,(5412.43+1348.23\,s+677.\,s^2) = 0$$

Short Period Natural Frequency:

$$\omega_{n_{SP}} \approx \sqrt{\frac{Z_\alpha M_q}{U_1} - M_\alpha} = 2.82749$$

Short Period Damping Ratio:

$$\zeta_{SP} \approx \frac{-\left(M_q + \frac{Z_\alpha}{U_1} + M_{\dot{\alpha}}\right)}{2\,\omega_{n_{SP}}} = 0.352162$$

3.5 Phugoid Approximation

3.5.1 Obtaining the formulas for Phugoid Approximation

For the Phugoid approximation, it is assumed α is constant with u and θ (or q) as the motion variables. It can be eliminated the α(s) terms and the moment equation to yield two equations with two motion variables.

$$\begin{pmatrix} (s - X_u - X_{T_u}) & g\cos\Theta_1 \\ -Z_u & [-(Z_q + U_1)\, s + g\sin\Theta_1] \end{pmatrix} \begin{pmatrix} u(s) \\ \theta(s) \end{pmatrix} = \begin{pmatrix} X_{\delta_e} \\ Z_{\delta_e} \end{pmatrix} \delta_e(s)$$

It is assumed that $\boxed{X_{\delta e} = Z_q = \Theta_1 \approx 0}$ and then the new form of equation comes to:

$$\begin{pmatrix} (s - X_u - X_{T_u}) & g \\ -Z_u & U_1 s \end{pmatrix} \begin{pmatrix} u(s) \\ \theta(s) \end{pmatrix} = \begin{pmatrix} 0 \\ Z_{\delta_e} \end{pmatrix} \delta_e(s)$$

The characteristic equation becomes

$$-U_1 \left(s^2 - (X_u + X_{T_u})\, s - \frac{Z_u}{U_1} g \right) = 0$$

$$\frac{u(s)}{\delta_e(s)} = \frac{\mathrm{Det}\left[\begin{pmatrix} X_{\delta_e} & g*\mathrm{Cos}[\theta_1] \\ Z_{\delta_e} & (-(Z_q + U_1)\, s + g*\mathrm{Sin}[\theta_1]) \end{pmatrix}\right]}{\mathrm{Det}\left[\begin{pmatrix} (s - X_u - X_{T_u}) & g*\mathrm{Cos}[\theta_1] \\ -Z_u & (-(Z_q + U_1)\, s + g*\mathrm{Sin}[\theta_1]) \end{pmatrix}\right]}$$

(Eq. 3.4a)

$$\frac{\theta(s)}{\delta_e(s)} = \frac{\mathrm{Det}\left[\begin{pmatrix} (s - X_u - X_{T_u}) & X_{\delta_e} \\ -Z_u & Z_{\delta_e} \end{pmatrix}\right]}{\mathrm{Det}\left[\begin{pmatrix} (s - X_u - X_{T_u}) & g*\mathrm{Cos}[\theta_1] \\ -Z_u & (-(Z_q + U_1)\, s + g*\mathrm{Sin}[\theta_1]) \end{pmatrix}\right]}$$

(Eq. 3.4b)

Table 3.3: Transfer Functions for Phugoid Approximation

3.5.2 Obtaining the numerical results for Phugoid Approximation

$\frac{u(s)}{\delta_e(s)}$ Using the Equation 3.4a, it is found:

$$\frac{1133.96}{-4.44233 - 13.295\,s - 675.138\,s^2}$$

$\frac{\theta(s)}{\delta_e(s)}$ Using the Equation 3.3b, it is found:

$$\frac{-0.694045 - 35.2446\,s}{-4.44233 - 13.295\,s - 675.138\,s^2}$$

Characteristic equation

$$-U_1\left(s^2 - (X_u + X_{T_u})\,s - \frac{Z_u}{U_1}\,g\right)$$

$$-677\,(0.00656179 + 0.0196922\,s + s^2)$$

In simplified form

$$-4.44233 - 13.3316\,s - 677.\,s^2$$

Phugoid Natural Frequency:

$$\omega_{n_{PH}} \approx \sqrt{\frac{-Z_u g}{U_1}} = 0.0810049$$

Phugoid Damping Ratio:

$$\zeta_{PH} \approx \frac{-(X_u - X_{T_u})}{2\,\omega_{n_{PH}}} = 0.117358$$

4. BODE DIAGRAMS

The Bode Diagrams created via Matlab (See Appendix A for codes) are listed below:

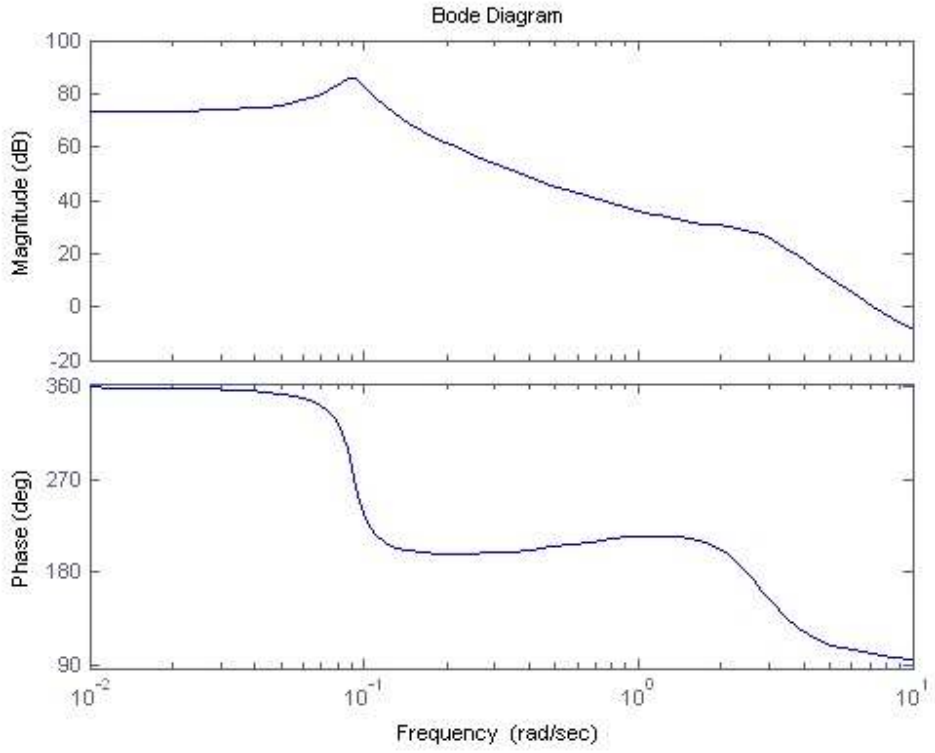

Figure 4.1: Bode Diagram of transfer function, u(s) / δ_e(s)

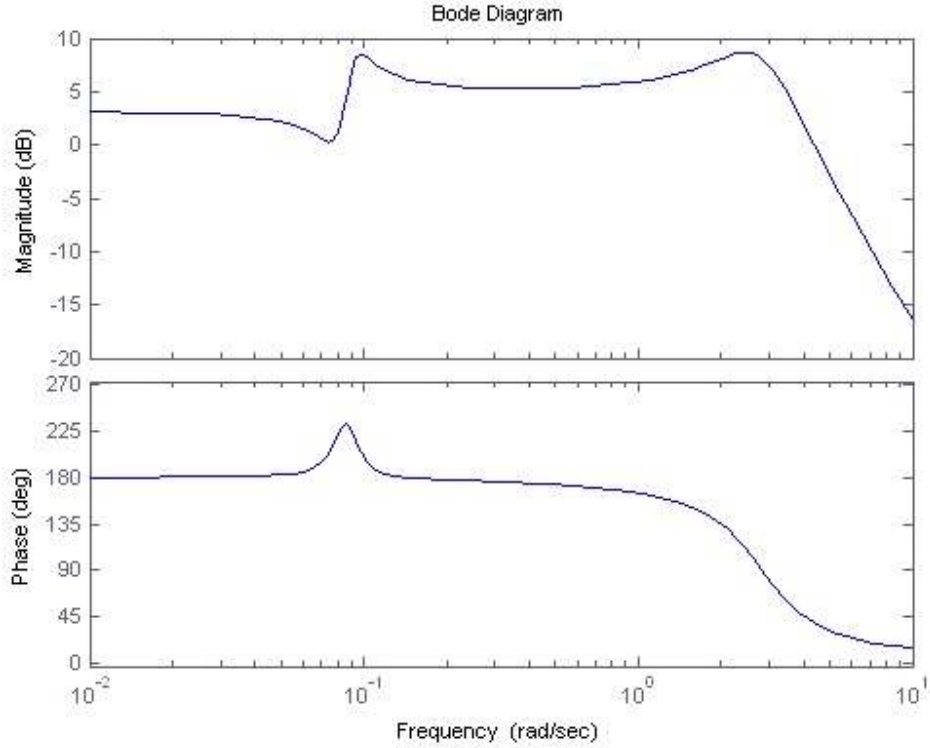

Figure 4.2: Bode Diagram of transfer function, α (s) / δ_e(s)

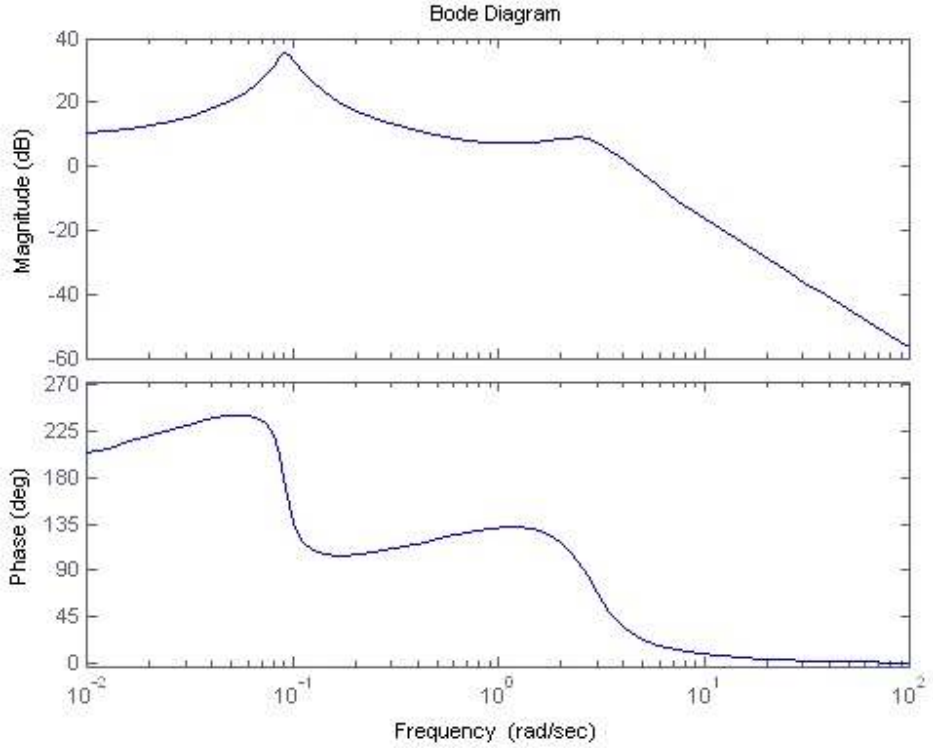

Figure 4.3: Bode Diagram of transfer function $\theta(s)/\ \delta_e(s)$

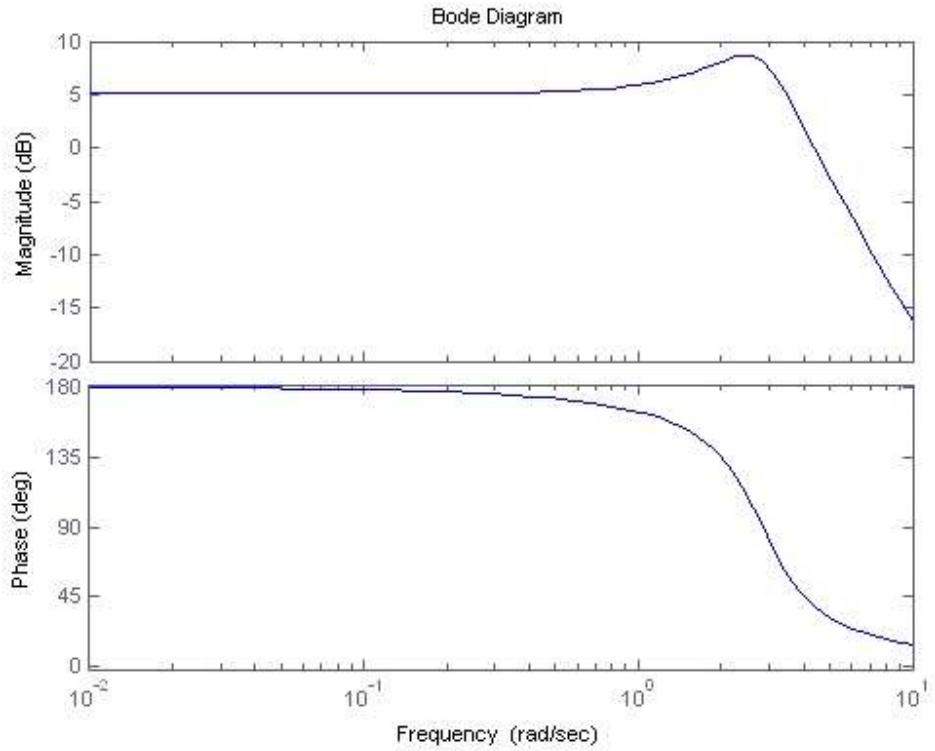

Figure 4.4: Bode Diagram of $\alpha(s)$ / $\delta_e(s)$ Using Short Period Approximation

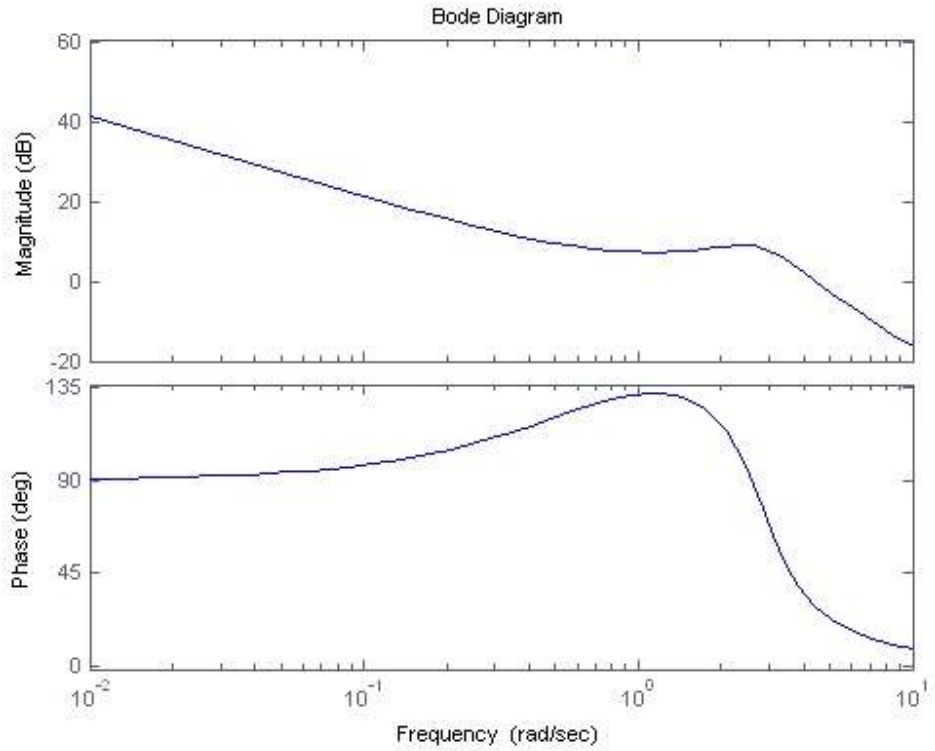

Figure 4.5: Bode Diagram of $\theta(s)/\delta_e(s)$ Using Short Period Approximation

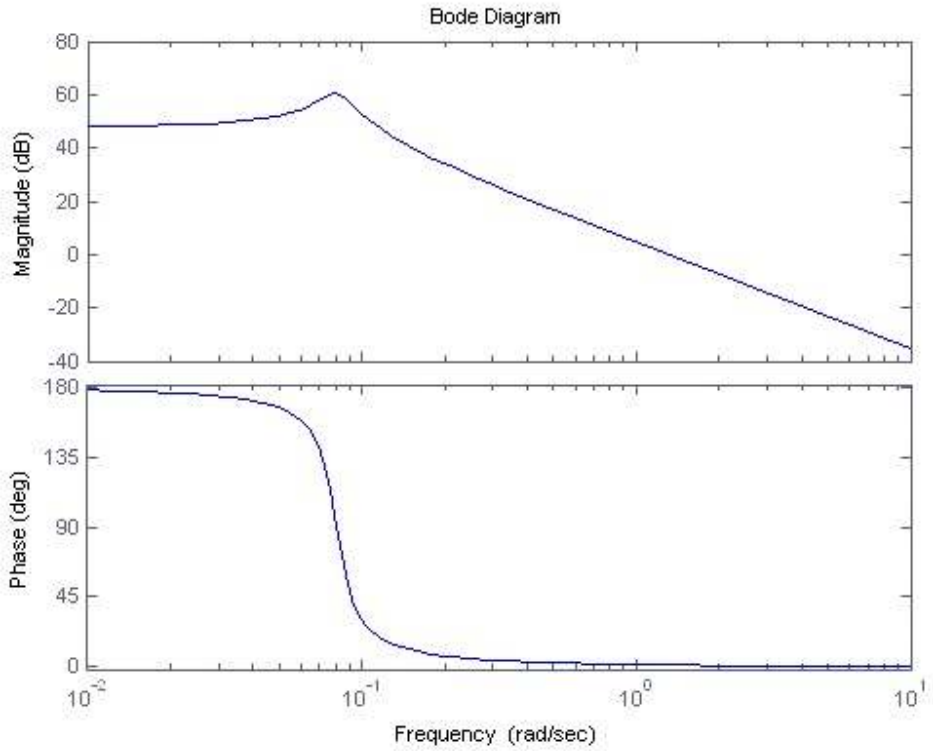

Figure 4.6: Bode Diagram of u(s)/ δ_e(s) Using Phugoid Period Approximation

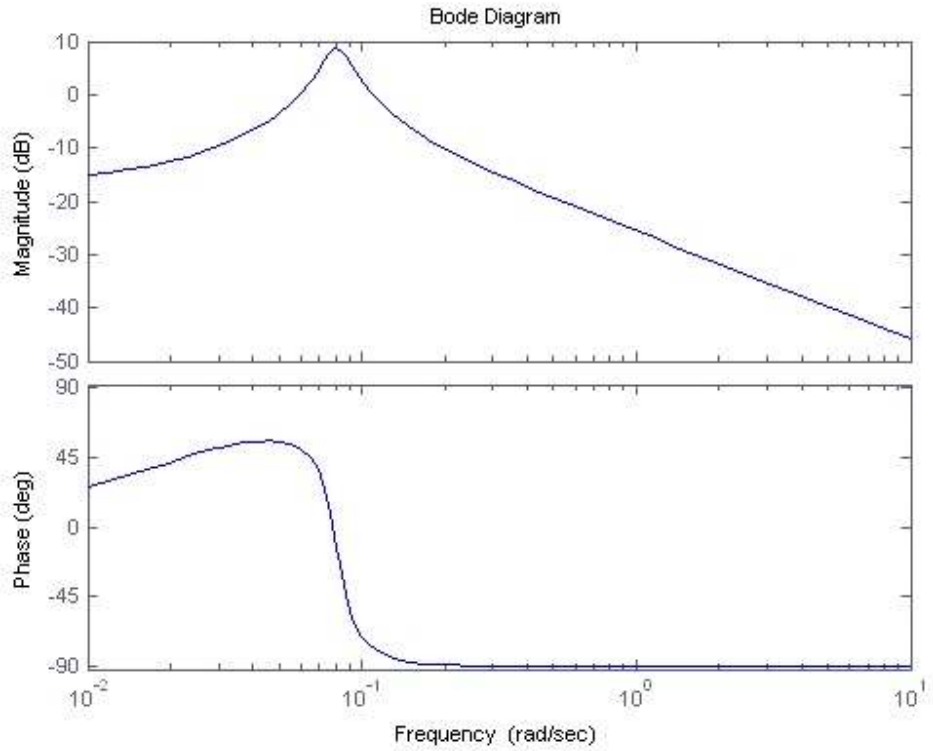

Figure 4.7: Bode Diagram of $\theta(s)/\delta_e(s)$ Using Phugoid Period Approximation

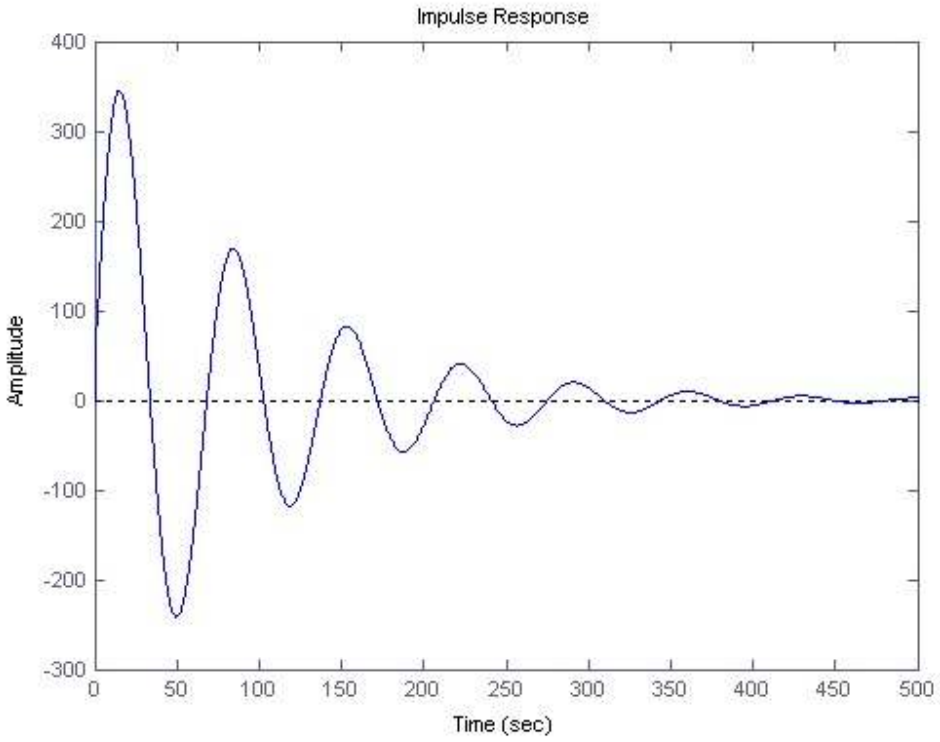

Figure 4.8: Transient Response Diagram of u(s) / δ_e(s)

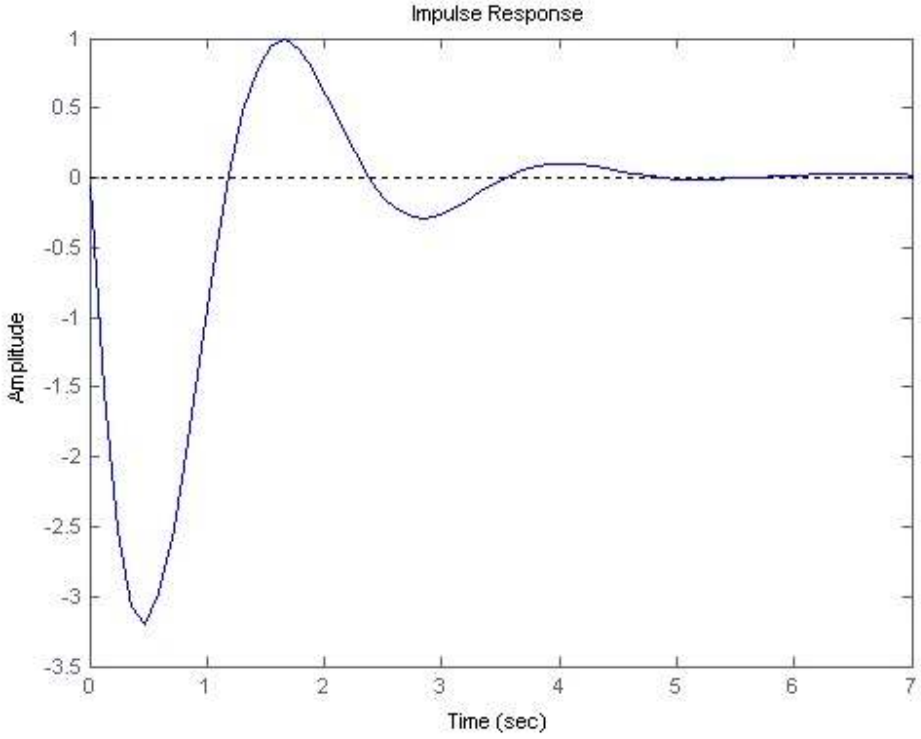

Figure 4.9: Transient Response Diagram of $\alpha(s) / \delta_e(s)$

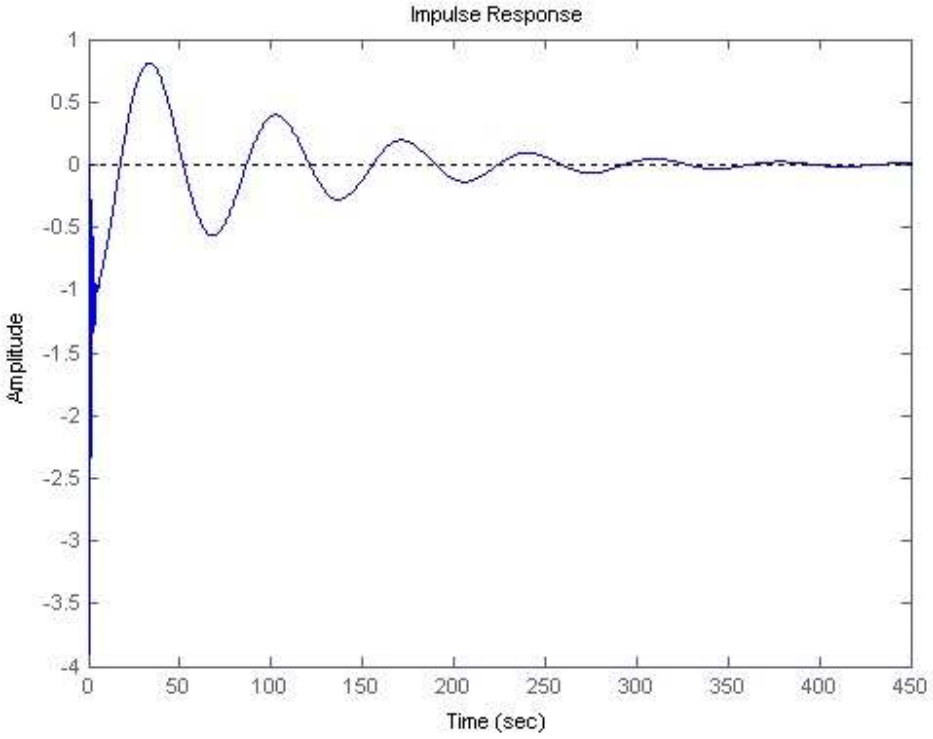

Figure 4.10: Transient Response Diagram of $\theta(s)/\ \delta_e(s)$

5. Conclusion

The short period mode is characterized by complex conjugate roots with a moderate to relatively high damping ratio and relatively high natural frequency and damped frequency. It is easily demonstrated by first trimming the aircraft and then disturbing it from trim with a forward aft neutral pitch.

The phugoid mode is characterized by complex conjugate roots with a relatively low damping ratio and neutral damped frequency (long period). It is demonstrated by trimming the aircraft in level flight, and then inputting aft.

It is also worthwhile to plot the short period and phugoid roots.

The short period roots are further out from the origin and have a higher damping ratio than the phugoid roots.

6. References

Yechout T.R. *Introduction to aircraft flight mechanic*, AIAA Education Series: Virginia, 2003

Caferov E. *Lecture Notes,* Istanbul, 2006

Etkin B., Reid L.D *Dynamics and Flight – Stability and Control,* New York, 1996

Blakelock J. *Automatic Control of Aircraft and Missiles,* Wiley: New York, 1991

Boyne, Walter J. *The Leading Edge*. New York: Stewart, Tabori & Chang, 1986.

Christy, Joe. *The Learjet*. Blue Ridge Summit, PA: Tab Books, 1979.

Pattillo, Donald M. *A History in the Making - 80 Turbulent Years in the American General Aviation Industry*. New York: McGraw-Hill, 1998.

Online Sources:

Bombardier Learjet. http://www.learjet.bombardier.com/en/3_0/3_2/3_2_0.jsp.

Gates Learjet 23. National Air and Space Museum.
http://www.nasm.edu/nasm/aero/aircraft/gates.htm

Learjet Company History. http://www.gretemangroup.com/learjet/history.html

National Aviation Hall of Fame Enshrinee Page – William Powell Lear, Sr.
http://www.nationalaviation.org/enshrinee/lear.html

Outstanding Aircraft Built by the Big 4: Bombardier/Learjet Aircraft Company. Wings Over Kansas. http://www.wingsoverkansas.com/extras/Learjet.html

Zimmerman, John. *The Learjet: Bill Lear's Greatest Idea.*
http://www.aircraftbuyer.com/featured/learjet.htm

Roskam Coefficients
http://www.megginson.com/Aviation/roskam-coefficients.html

http://avstop.com/AC/FlightTraingHandbook/ LongitudinalStability.html

www.wikipedia.com

A. Appendix #1 – Matlab Codes

Statements:

```
g=tf([-297.043,229678,199768],[677.871,1361.64,5426.41,122.884,45.1686]);
g2=tf([-35.2446,-9683.25,-190.671,-64.4613],[677.871,1361.64,5426.41,122.884,45.1686]);
g3=tf([-9675.1,-6399.5,-139.155],[677.871,1361.64,5426.41,122.884,45.1686]);
h1=tf([-0.05206,-14.3415],[1,1.99147,7.99473])
h2=tf([-14.2726,-9.17132],[1,1.99147,7.99473,0]);
f1=tf([1133.96],[-675.138,-13.295,-4.44233])
f2=tf([-35.2446,-0.694045],[-675.138,-13.295,-4.44233])
```

Plotting:

```
bode(g2,{0.01,10})
bode(g,{0.01,10})
bode(g3,{0.01,100})
bode(h1,{0.01,10})
bode(h2,{0.01,10})
bode(f1,{0.01,10})
bode(f2,{0.01,10})
impulse(g)
impulse(g2)
impulse(g3)
```